CHIN.PHYS.LETT. Vol. 25, No. 9 (2008) 3429

Acoustic Imaging Frequency Dynamics of Ferroelectric Domains by Atomic Force Microscopy *

ZHAO Kun-Yu(赵坤宇)[1], ZENG Hua-Rong(曾华荣)[1]*, SONG Hong-Zhang(宋红章)[1], HUI Sen-Xing(惠森兴)[1], LI Guo-Rong(李国荣)[1], YIN Qing-Rui(殷庆瑞)[1], Kiyoshi Shimamura[2], Chinna Venkadasamy Kannan[2], Encarnacion Antonia Garcia Villora[2], Shunji Takekawa[2], Kenji Kitamura[2]

[1]*State Key Lab of High Performance Ceramics and Superfine Structures, Shanghai Institute of Ceramics, Chinese Academy of Sciences, Shanghai 200050*

[2]*Optronic Materials Center, National Institute for Materials Science, 1-1 Namiki, Tsukuba, Ibaraki 305-0044, Japan*

(Received 23 June 2008)

We report the acoustic imaging frequency dynamics of ferroelectric domains by low-frequency acoustic probe microscopy based on the commercial atomic force microscopy. It is found that ferroelectric domain could be firstly visualized at lower frequency down to 0.5 kHz by AFM-based acoustic microscopy. The frequency-dependent acoustic signal revealed a strong acoustic response in the frequency range from 7 kHz to 10 kHz, and reached maximum at 8.1 kHz. The acoustic contrast mechanism can be ascribed to the different elastic response of ferroelectric microstructures to local elastic stress fields, which is induced by the acoustic wave transmitting in the sample when the piezoelectric transducer is vibrating and exciting acoustic wave under ac electric fields due to normal piezoelectric effects.

PACS: 77. 84. -s, 77. 84. Dy, 77. 80. Dj, 07. 78. +s, 07. 79. Lh

Scanning probe microscopy has become an increasingly powerful tool to characterize nanoscale structures physical properties of various materials and potential technological applications.[1] Very recently, scanning near-field ultrasound holography has been explored to provide nanoscale-resolution images of internal substructures of microelectronic materials and malaria parasites in red blood cells.[2] In ferroelectric fields, nanoscale domain structure of ferroelectric thin films, ceramics and single crystals can be imaged and controlled directly using piezoresponse force microscopy.[3−10] In addition, acoustic mode scanning force microscopy, including atomic force acoustic microscopy,[11−12] ultrasonic force microscopy,[13−16] and scanning probe acoustic microscopy,[17] has the advantage of visualizing nanoscale domain structures, elastic properties or subsurface configurations, with an operating frequency ranging from a few 100 kHz to 1 MHz. In our previous study, low-frequency acoustic probe microscopy based on the commercial AFM was developed and successfully used to image ferroelectric domains in relaxor-type ferroelectric $PbMg_{1/3}Nb_{2/3}O_3$–$PbTiO_3$ single crystals and elastic structures in the lead-free $Bi_4Ti_3O_{12}$ piezoelectric ceramics.[18,19] Fingerprint domain configurations were clearly visualized by such low-frequency acoustic microscopy at the frequency down to 6.42 kHz.[18] However, no investigation on the frequency-dependent domain imaging has been carried out for acoustic microscopy so far. In this Letter, acoustic imaging frequency dynamics of ferroelectric domain is reported by using such a low-frequency acoustic microscopy.

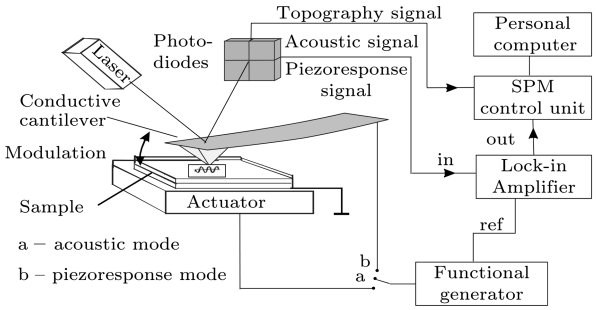


Fig. 1. Schematic diagram of low-frequency acoustic probe microscopy incorporated with a PFM.

Figure 1 shows the schematic sketch of the customer-built low-frequency near-field acoustic probe microscopy based on the commercial atomic force microscope (AFM) (Seiko Inc. Japan) operating in acoustic mode (a), in which a piezoelectric transducer was bonded onto a sample holder of an AFM, and the sample was glued on the transducer. An external function generator provides sinusoidal excitation signals applied to the piezoelectric transducer, which gives rise to flexural vibration and thereby excites acoustic waves into the sample, causing a periodic local deformation of the sample surface underneath the tip. The motion of the scanning force microscopy tip is detected optically by laser beam deflection from the backside of the cantilever. The detected signal is then fed to a lock-in amplifier for imaging. Figure 1 also includes

*Supported by the National High-Technology Research and Development Programme of China under Grant No 2007AA03Z330, the National Natural Science Foundation of China under Grant No 10774113, and the Innovation Project of the Shanghai Institute of Ceramics (SCX-0612).

**Email: huarongzeng@mail.sic.ac.cn

© 2008 Chinese Physical Society and IOP Publishing Ltd

the setup of piezoresponse mode AFM (b), which is used to obtain the piezoresponse signal of ferroelectric domains corresponding to those detected in acoustic mode. The specimens for the present investigation include ferroelectric (Pb,La)(Zr,Ti)O_3 (PLZT) ceramics prepared by the conventional solid state reaction and $BaMgF_4$ (BMF) single crystal grown from the melt by Czochralski technique. The specimens were polished to optical grade with a thickness of 120 μm.

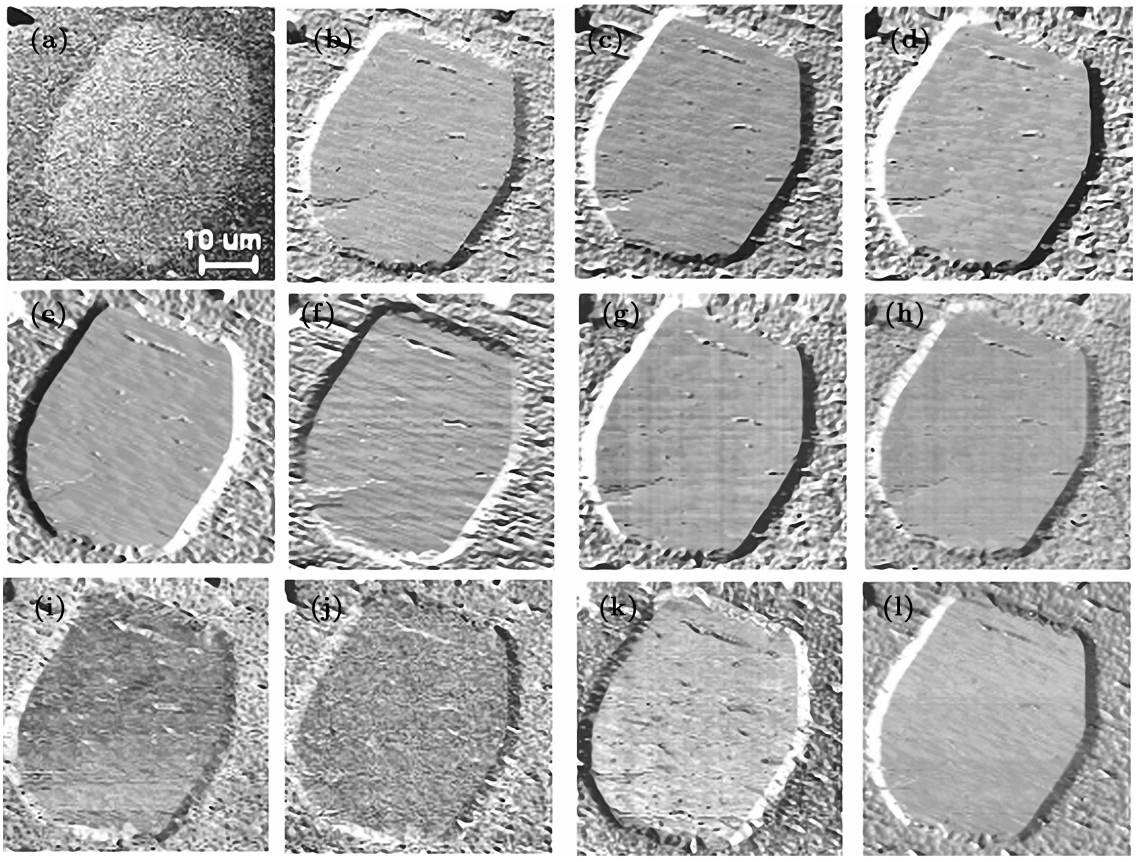


Fig. 2. Piezoresponse image ((a) the imaging ac frequency 8.1 kHz) and corresponding acoustic images of a ferroelectric domain in $BaMgF_4$ crystal at 1 kHz (b), 2 kHz (c), 7.7 kHz (d), 8.1 kHz (e), 10 kHz (f), 20 kHz (g), 40 kHz (h), 60 kHz (i), 80 kHz (j), 100 kHz (k) and 132 kHz (l).

Figure 2 shows the piezo-response image of one isolated, hexagonal domain in the ferroelectric $BaMgF_4$ single crystal and corresponding acoustic images taken in a broad frequency range from 1 kHz to 132 kHz. The bright and dark piezoresponse contrast reveals antiparallel polarization state due to out-of-phase piezoelectric vibration under the ac field applied between the AFM tip and the sample bottom electrode, while the acoustic images show remarkably different contrast at different frequencies. It can be clearly seen that the acoustic images depicted in Figs. 2(b)–2(d) display convex structures at 1 kHz, 2 kHz, and 7.7 kHz. With the increasing modulation frequency from 8.1 kHz to 10 kHz, the convex structure changes to concave shape in the acoustic image (see Figs. 2(e)–2(f)). Such acoustic configuration change continues at higher frequency, as shown in Figs. 2(g)–2(l). The acoustic image of the hexagonal domain appears convex pattern at 20 kHz (Fig. 2(g)), 40 kHz (Fig. 2(h)), 60 kHz (Fig. 2(i)), and 80 kHz (Fig. 2(j)), and shows concave structure at 100 kHz (Fig. 2(k)), while it reappears as convex pattern at 132 kHz (Fig. 2(l)). In addition, another interesting phenomenon could be found if we compare the piezoresponse image with the acoustic ones. It must be noted that the acoustic image shows more stereo than the corresponding piezoresponse one. Such features reveal that the acoustic signal at a low frequency is stronger than that at a high frequency due to remarkable decrease of ferroelectric indentation nearby the tip at the low frequency. While higher tip indentation forces possibly occur at high frequency, reducing the contrast of the acoustic image due to inhibiting acoustic signal excitation and measurement.

The visualized acoustic image contrast in Fig. 2 could be understood from the point view of interaction between the excited acoustic wave and microstructures in the sample. In the low-frequency acoustic microscopy, the sample vibration is modulated sinusoidally in time by the underneath ac field-excited

transducer. The tip vibrates in phase with the sample surface displacement due to low frequency modulation. The modulated tip amplitude reflects actually the tip-sample surface interaction stiffness (contact stiffness k^*). Supposing that the tip-surface contact obeying the Hertzian contact-mechanics model,[20] k^* can be expressed as

$$k^* = \sqrt[3]{6E^{*2}RF}, \tag{1}$$

where R is the radius of the tip apex, F the applied load by tip to the sample surface, E^* the reduced elastic modulus of the tip-sample surface system. E^* could be expressed as

$$\frac{1}{E^*} = \frac{1-\nu_s^2}{E_1} + \frac{1-\nu_c^2}{E_2}, \tag{2}$$

where E_1, E_2 and ν_s, ν_c are the Young's moduli and the Poisson's ratio of the surface and the cantilever, respectively. It is clear that the value of k^* depends not only on the applied static load and the tip geometry, but also on the elastic properties of the tip and the sample. For the ferroelectric material, k^* is additionally related to the interaction between the local ferroelectric microstructure (ferroelectric domain) beneath the tip and the excited acoustic wave in the bulk sample. It is well known that the bulk electric polarization due to a preferred macroscopic orientation of the domains influences the elastic response of a ferroelectric material when stresses are applied.[21] Thus, in the case of ferroelectric BMF single crystal, the acoustic contrast reflects contact stiffness difference of ferroelectric domains depending on the local elastic field-induced acoustic vibration in the sample during imaging at low frequency.

Burnham *et al.* proposed a rheological model to explain the AFM tip-sample interaction in the transducer-driven sample vibration configuration,[22] in which the dynamic behaviour for the relationship between the tip position (d) and transducer position (z) can be expressed as

$$\frac{d}{z} = \frac{k^*\left[1+\left(2m^*\omega\beta^*/k^*\right)^2\right]^{1/2}}{\sqrt{(k^*+k_c-m^*\omega^2)^2+\left[2m^*\omega\left(\beta^*+\beta_c\right)\right]^2}}, \tag{3}$$

where the cantilever is described by spring stiffness k_c, damping constant β_c and effective mass m^*. The tip-sample interaction stiffness is $k^*(z,d)$ and its damping is $\beta^*(z,d)$. The above equations postulate both factors to determine the acoustic signal and the existence of peak frequency of the acoustic excitation. It can be clearly seen that the dynamical frequency dependence of the tip position is generally governed by the factors including the interaction contact stiffness between the tip-cantilever system and the sample surface, the elasticity of the cantilever-tip system and their damping factors. These complex factors determine the acoustic amplitude and the phase shift, thus give rise to the observed acoustic pattern change (convex to concave). It is very difficult to give a quantitative description of the acoustic frequency dynamics observed in Fig. 2. However, one can roughly expect stronger acoustic signal contrast at low frequency. According to Eq. (3), an acoustic response peak is expected in the tip displacement-frequency dynamic behaviour, as demonstrated by Burnham *et al.*[22] Our experimental result shows that this maximum acoustic response appears at 8.1 kHz in the modulation frequency dependence of the measured acoustic amplitude signal (Fig. 3(a)). The inset in Fig. 3(a) shows that the acoustic signal becomes stronger mainly at the frequencies ranging from 7 kHz to 10 kHz, and nearly degrades to a constant for the frequency beyond 20 kHz. Such behaviour is clearer in the logarithmic plot of the acoustic signal as a function of the modulation frequency (Fig. 3(b)), where the log-signal fits a linear-frequency dependence on both sides of the peak frequency. This quantitative measurement demonstrates the acoustic microscopy valid in imaging ferroelectric domains at low frequency.

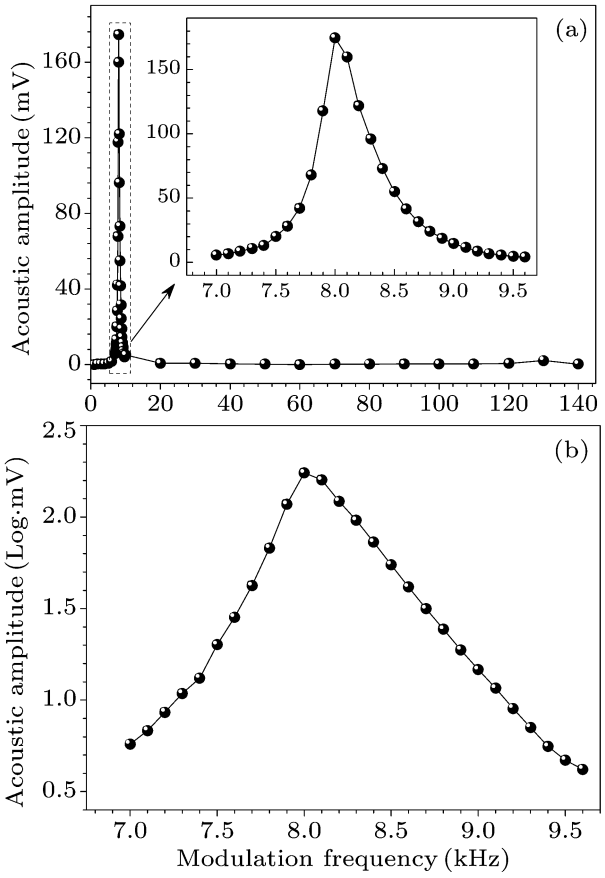


Fig. 3. (a) Modulation frequency dependence of the acoustic amplitude signal of ferroelectric domains in BaMgF4 single crystal. Inset: the acoustic signal in the frequency ranging from 7 kHz to 10 kHz, (b) the logarithmic plot of the acoustic signal as a function of the modulation frequency for inset of Fig. 3(a).

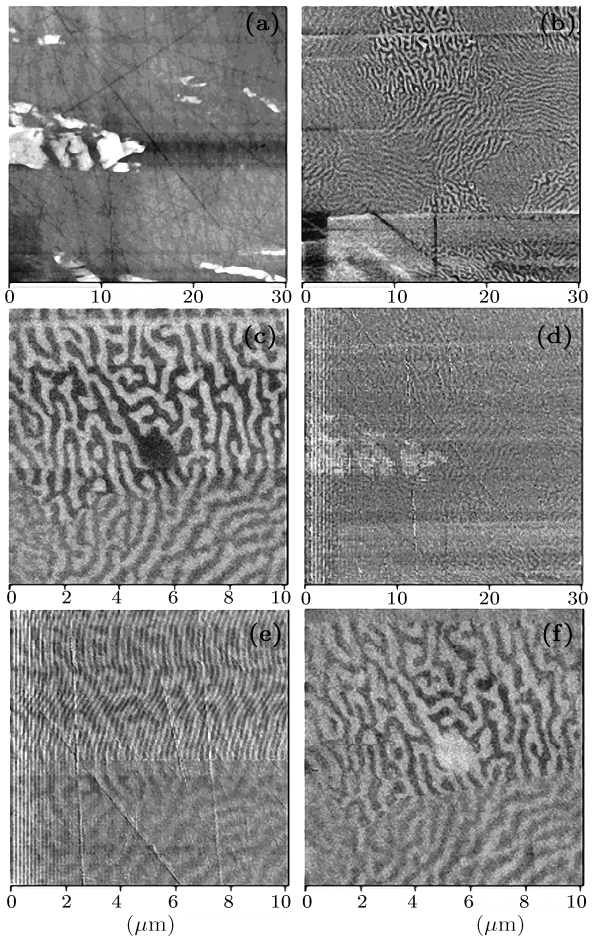


Fig. 4. Topography image (a) of ferroelectric PLZT ceramics, its corresponding piezoresponse image [(b) and (c)] at 9.3 kHz, the acoustic image [(d) and (e)] at 0.5 kHz and (f) at 9.3 kHz. The scanning area of $30 \times 30\,\mu m^2$ for [(a), (b) and (d)] are the same, and the same area of $10 \times 10\,\mu m^2$ for [(c), (e) and (f)].

To further illustrate the frequency-dependency of acoustic signal, we focus on acoustically imaged domains of ferroelectric PLZT ceramics at lower frequency, as shown in Fig. 4. Figures 4(d) and 4(e) are acoustic images of ferroelectric domains in PLZT sample at ultra-low frequency down to 0.5 kHz. Although the domain patterns show some vague due to the disturbs from the ambient at such low frequency, the fingerprint domain patterns are still in agreement well with the piezoresponse image of Figs. 4(b) and 4(c) at 9.3 kHz. The acoustic image at 9.3 kHz (Fig. 4(f)) becomes more clear than that at 0.5 kHz (Figs. 4(d) and 4(e)). Compared with other AFM-based acoustic microscopies such as atomic force acoustic microscopy (AFAM),[11] ultrasonic force microscopy (UFM)[13] and scanning near-field ultrasound holography[2] operating at high frequency ranging from several hundreds of kHz to a few MHz, our present acoustic microscopy offers superhigh resolution, ultra-low imaging frequency and remarkably resolved image as well. Especially for observing ferroelectric domains, such low-frequency acoustic microscopy shows unique imaging features than UFM by Tsuji *et al.*,[13] in which the ultrasonic imaging of PZT ceramics exhibits a blurry domain boundary at high frequency close to 500 kHz.

It is interesting to find that ferroelectric domains visualized by AFM-based acoustic microscopy at such lower frequency. An in-depth analysis concerning the physical mechanism of acoustic imaging is necessary in the further work. Although the present low-frequency acoustic microscopy demonstrates high resolution imaging capability,[19] it so far only limits to ferroelectrics. Based on the interaction between the acoustic wave and microstructures in the specimen, a detailed investigation could be made to detect microelectronic in the semiconductor and cell structural of bio-systems, respectively.

In summary, a low-frequency acoustic probe microscopy based on the commercial AFM has successfully applied to study ferroelectric domains excited by ultra-low frequency acoustic signal. Ferroelectric domain could be observed at frequency down to 0.5 kHz. The frequency-dependent acoustic signal reveals a strong acoustic response in the frequency range from 7 kHz to 10 kHz, and reaches the maximum at 8.1 kHz. The acoustic signal contrast mechanism can be ascribed to the different elastic response of ferroelectric microstructures to local elastic stress fields, which is induced by the acoustic wave transmitting in the sample when the piezoelectric transducer excites acoustic waves under ac electrical bias due to normal piezoelectric effects. This low-frequency acoustic microscopy is expected to demonstrate a powerful promising tool for nondestructive, high resolution, real-space imaging of microstructures in ferroelectric material and biological systems.

References

[1] Loos J 2005 *Adv. Mater.* **17** 1821
[2] Shekhawat G S and Dravid V P 2005 *Science* **310** 89
[3] Gruverman A et el 1998 *Annu. Rev. Mater. Sci.* **28** 101
[4] Nagarajan V et el 2003 *Nature Mater.* **2** 43
[5] Molotskii M et el 2003 *Phys. Rev. Lett.* **90** 107601
[6] Terabe K et el 2003 *Appl. Phys. Lett.* **82** 433
[7] Kalinin S V 2004 *Phys. Rev.* B **70** 184101
[8] Bai F M et el 2004 *Appl. Phys. Lett.* **85** 2313
[9] Scrymgeour D and Gopalan V 2005 *Phys. Rev.* B **72** 024103
[10] Paruch P et el 2005 *Phys. Rev. Lett.* **94** 197601
[11] Rabe U et el 2002 *J. Phys. D.: Appl. Phys.* **35** 2621
[12] Hurley D C et el 2002 *Meas. Sci. Technol.* **16** 2167
[13] Tsuji T, Ogiso H, Akedo J, Saito S, Fukuda K and Yamanaka K 2004 *Jpn. J. Appl. Phys.* **43** 2907
[14] Kolosov O V et el 1998 *Phys. Rev. Lett.* **81** 1046
[15] Inagaki K et el 2000 *Appl. Phys. Lett.* **76** 1836
[16] Matsuda O et el 2002 *Jpn. J. Appl. Phys.* **41** 3545
[17] Liu X X et el 2002 *J. Phys.* D **35** 74
[18] Zeng H R et el 2005 *Solid State Commun.* **133** 521
[19] Zeng H R et el 2005 *Phys. Status Solidi* **202** R41
[20] Hertz H J 1882 *J. Reine Angew. Math.* **92** 156
[21] Moulson A and Herbert J M 1990 *Electroceramics* (London: Chapman and Hall)
[22] Burnham N A et el 1996 *J. Vac. Sci. Technol.* B **14** 1308